Tellus (1995), 47A, 629–637
Printed in Belgium – all rights reserved

TELLUS
ISSN 0280–6495

On the mechanism of cyclogenesis as deduced from vertical axis tilts

By RICHARD GROTJAHN*, *Department of Land, Air, and Water Resources, University of California, Davis, CA, 95616, USA* and JOSEPH TRIBBIA, *National Center for Atmospheric Research*†, *Boulder, CO, 80307, USA*

(Manuscript received 22 August 1994; in final form 16 January 1995)

ABSTRACT

The relative strengths of 2 mechanisms to explain early stages of cyclogenesis are examined with an initial value model. Either mechanism can be emphasized by different choices of initial trough axis configuration. In our model, if initial conditions have an upper level trough upstream of the surface trough, and both troughs have little tilt, the growth is primarily by normal mode instability. Some evidence is presented suggesting that observed troughs are initially separate and have little along-flow tilt. A case study is shown where an observed storm develops while maintaining a fixed structure for a short period of time. The evidence suggests that the normal mode concept is a relevant motif for cyclogenesis.

1. Introduction

Several mechanisms have been proposed to govern cyclogenesis. Davis and Emanuel (1991) illustrate three of these mechanisms from the perspective of potential vorticity (PV). In the first mechanism, PV anomalies at different levels in the atmosphere are displaced in such a way as to make each other grow and keep each other in step (Hoskins et al., 1985). This mechanism is closest to the traditional normal mode baroclinic instability (Grotjahn, 1980) in which the reinforcement is coherently maintained (Bishop, 1993), and we shall call it NMBI. The phase displacement remains fixed. All properties of the eddy grow in NMBI. The second mechanism generates growth in some eddy properties by increasing the positive reinforcement of superimposed PV anomalies. Non-normal mode structures (e.g. freely advecting potential vorticity perturbations in the Eady problem) can comprise an initial condition (in addition to normal modes) and this mechanism operates by phase shifting PV anomalies. We call this mechanism nonmodal growth, or NG. In the absence of favorably configured deformation in the basic state, NG is transient but can be quite large (Farrell, 1984). These two mechanisms can be illustrated using adiabatic dynamics. The third mechanism allows diabatic processes (such as latent heat release in convection) to generate an internal PV anomaly that interacts with other PV present (Davis and Emanuel, 1991). This study focuses on the relative merits of the first two mechanisms: NMBI and NG.

One motivation for considering NMBI and NG concerns the ability of NG to generate much more rapid growth than NMBI under certain circumstances. Theoretical work shows that NG can be very large when the initial condition includes a large amount of against-shear vertical tilt in the trough and ridge axes. As the tilt is reduced, the thermal part of the potential vorticity is converted into the kinetic part (i.e., relative vorticity) (Grotjahn et al., 1994.) This property is claimed to illustrate the observed approach of an upper level trough to a surface feature during cyclogenesis. A simplified analytic analysis (Grotjahn et al., 1994) suggests that NG would be greatly reduced

* Corresponding author.
† The National Center for Atmospheric Research is sponsored by the National Science Foundation.

if the upper and lower features were separate and each had little tilt (instead of one trough *connected* through the entire troposphere). In Section 2 we use a simple theoretical model to illustrate this point.

Given the strong sensitivity of NG to the initial pattern of trough axes, it is worthwhile to examine observed trough axes. Are observed troughs steeply tilted prior to development? Does the separation between upper and lower features diminish continuously or is there a period that could be identified as having a fixed structure? In Section 3 we reexamine previous work and present our case study when considering these two questions.

2. Theoretical studies

Imagine two types of initial conditions, illustrated schematically in Fig. 1. In both cases, the initial separation between the troughs at the tropopause and surface levels is the same. In one case (Fig. 1a) the upper and lower trough are connected, resulting in a large, against-shear vertical tilt. As the integration proceeds, this trough axis becomes more vertical. Nonmodal growth occurs at each stage. The mechanism can be understood from the standpoint of quasi-geostrophic potential vorticity, Q. Since Q is conserved, relative vorticity is growing to match the net decline in the remainder of Q caused by a diminished tilt that decreases vertical derivatives of stream function. To illustrate "pure" NG, this example is assumed to have no unstable normal mode.

In Fig. 1b, a different initial condition is shown. In this case the upper and lower troughs are separate and interior Q is primarily relative vorticity. As the integration proceeds, there is assumed to be negligible NG and the normal mode baroclinic instability creates a negligible change in the total amplitude until the upper and lower troughs are separated by a distance $(S_1 - \tau_1)$ that approximates the phase separation of the growing normal mode. After that time NMBI occurs. Some properties of these highly idealized examples can be illustrated with our theoretical model.

It should be noted that NG can occur even when only normal modes are present (Müller et al., 1989; Rotunno and Fantini, 1989). In Grotjahn et al. (1994) we point out that the normal modes are a larger fraction of the total for strong NG when interior friction is included. In the present matter, recent studies by Bishop (1993) and Davies and Bishop (1994) are noteworthy. They express the Eady (1949) solution in terms of two edge waves in potential temperature (Θ). Once cast this way, they can go beyond the special case where the edge waves have a fixed phase shift given by the normal mode. They allow initial conditions where the two edge waves are separated by various distances and track the time evolution towards the growing normal mode. While they find NG occurring when the upper feature is catching up with the lower in most cases, they do find some long wave solutions for which the opposite occurs.

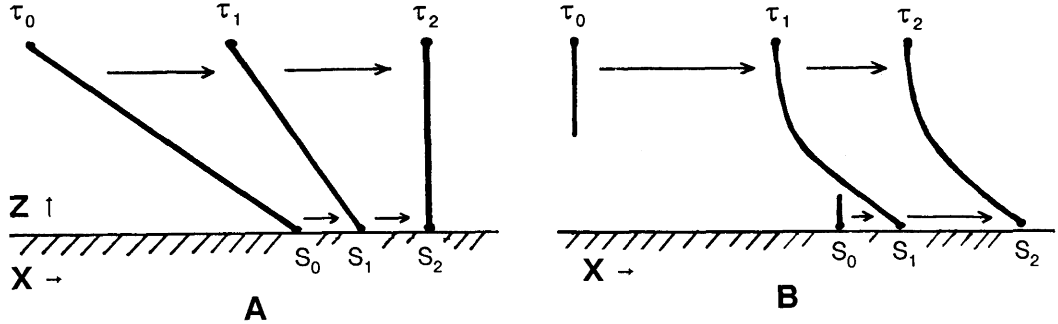

Fig. 1. Longitude-height cross sections showing idealized trough axes at successive times with end points marked S (surface) and τ (tropopause level). Subscripts denote time. (a) Example of NG. (b) Example of NMBI, where a fixed-shape normal mode dominates after time equals 1. Note that distances $S_0 - \tau_0$ and $S_1 - \tau_1$ are independent of the example.

It is not clear that those results of the Eady formulation, which neglects Coriolis variation and so is inappropriate for long waves, are applicable here.

The use of edge waves works well as an interpretative tool for the Eady model. However, in our model, it is not clear that a pair of edge waves are present, in particular there may not be a good analog to the upper edge wave in the Eady analysis. There is some discussion of this point in Davies and Bishop (1993, p. 1943). The basic state in our model does not have a tropopause break. We do not pursue an edge wave analysis further since our study is designed to see how the initial value problem evolves differently from a pure normal mode. We shall separate the growing normal mode from interactions (superpositions) of all the other modes with each other and with the growing normal mode. Thereby, we are making a link to the long history of studies that just examine the growing normal mode.

Our theoretical, initial value model is linear, quasi-geostrophic, and compressible. The equations are formulated in Cartesian geometry with linearly variable Coriolis, and variable static stability. The specified (mean flow) zonal velocity is independent of horizontal variation but is zero at the ground and maximum at tropopause level. Details are given in Grotjahn et al. (1994).

The schematic initial condition depicted in Fig. 1a is simulated by the model initial condition shown in Fig. 2a. Fig. 2b shows the corresponding time series of two growth rate parameters. The parameter labelled L_2' is the growth rate of

$$L_2 = \left(\frac{1}{N_{\text{pts}}} \sum_{n=1}^{N_{\text{pts}}} \rho \phi^2 \right)^{1/2}. \tag{1}$$

L_2 measures the density weighted amplitude. N_{pts} is the number of points in the 2-dimensional (longitude-height) domain that includes one wavelength and all vertical levels. A parameter, H is defined by an expression that is similar to the one for L_2 except $\rho\phi^2$ is replaced with Q^2 (potential enstrophy) and the square root is not taken. H' is the growth rate of H.

Both L_2' and H' asymptote to the normal mode growth rate given by NMBI. L_2' near the start of

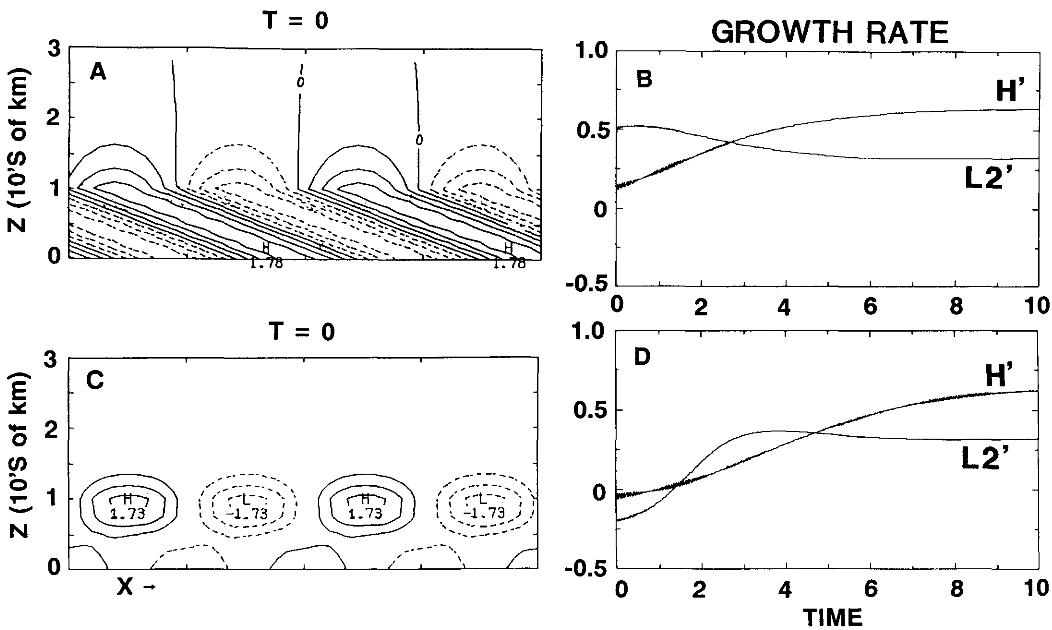

Fig. 2. Linear model simulation of idealized examples shown in Fig. 1. (a) Initial condition for connected and tilted axes in troposphere. (b) Nondimensional growth rates time series of RMS amplitude (L_2') and potential enstrophy (H') for initial condition shown in (a). (c) and (d) Initial condition for separate and vertical axes. Corresponding growth rates.

the integration exceeds the NMBI rate substantially, peak values of L_2' are almost double the NMBI rate. The distribution of H' tends to reflect just the growing normal mode. As the normal mode increases in amplitude it becomes a larger and larger fraction of the total Q. Thus, H' asymptotes steadily to twice the NMBI rate.

A measure of the fraction of the growing normal mode in the total solution is

$$F = \frac{\sum |\psi_{\mathrm{gnm}}|}{\sum |\psi_{\mathrm{gnm}}| + \sum |\psi_{\mathrm{t}} - \psi_{\mathrm{gnm}}|}, \tag{2}$$

where absolute values are summed over all N_{pts}. The stream function projected onto the growing normal mode is ψ_{gnm}, while the total stream function is ψ_{t}. For the connected trough, F is initially large (50%) and exceeds 90% during day 7.

Fig. 2c shows the model initial condition used to approximate the schematic given in Fig. 1b. The trough axes are separate and vertical initially. The corresponding growth rates are given in Fig. 2d. In contrast to the previous case, the NG mechanism is greatly reduced. This is evident by the lack of significant L_2 growth in excess of the normal mode rate. The upper feature does approach the lower feature but an against-shear tilt *develops* in each feature; the former change implies positive NG. The increasing upstream tilt might imply negative NG from the reasoning made in the introduction, since relative vorticity would go into the thermal part of the PV. Apparently, the NG mechanism is weak in this case. The negative L_2 growth rate at the start is due in part to the presence of a decaying normal mode in the initial condition. The growing normal mode is a much smaller fraction of the total in this initial condition. F is 30% at the start, reaches 50% at the start of day 3, and does not exceed 90% until the start of day 9. The time series of H' also implies that the period before the normal mode dominates is longer than in the prior case.

Table 1 summarizes how the normal mode fraction varies with different representative initial conditions. F is again used as the indicator. The variable p indicates how far upstream the trough at tropopause level is from the surface trough. Since a single wavenumber in the x direction is used, the separate, non-tilted troughs repeat initial conditions every 2 units of m. The line for $m = 1.5$ has the two cases shown in Figs. 2a, c. Depending on the case, m between 0.33 and 0.5 has a phase shift from surface to tropopause level that is closest to the normal mode. For larger upstream phase shift, the normal mode is a smaller fraction of the total.

Table 1. *F values for connected and unconnected initial conditions*

	Connected		Separate	
m	F(%)	p	F(%)	p
0	52.2	0	29.0	0
0.25	72.6	1/8	44.8	1/8
0.33	80.1	1/6	50.2	1/6
0.5	78.4	1/4	54.9	1/4
0.67	70.2	1/3	51.9	1/3
1.0	57.7	1/2	42.0	1/2
1.5	49.5	3/4	29.4	3/4
2.0	48.1	1	29.0	0
3.0	52.8	3/2	42.0	1/2

m is vertical wavenumber (connected troughs use $\exp(im\pi z)$; separate use $\exp(im\pi)$ for upper relative to lower trough). p is upstream shift in wavelengths from $z = 0$ to $z = 1$.

The visual appearance of the solution evolution is given in Grotjahn et al. (1993). The initial condition for the $m = 1.5$ separate troughs case is given in Fig. 2c. As time proceeds the phase shift, between the upper chain and the lower chain of highs and lows, diminishes while there is little change of amplitude. (Thus, small growth rates occur in Fig. 2d.) After about 3 units of time the phase shift is roughly $\frac{1}{2}$ wavelength, a noticeable westward tilt with height has developed in the middle troposphere, and the solution is rapidly growing. Fig. 2d is consistent with this description. At later times (e.g., day 7) the normal mode structure dominates, so further changes are primarly just amplification and propagation of a phase-locked structure.

Warrenfeltz and Elsberry (1989) have made a related series of calculations. Their study includes solutions from a "quasi-linear", adiabatic, 12-level, primitive equation model. For initial conditions, they specify upper and lower streamfunction perturbations that each contain no tilt. They vary the initial phase separation between the perturbations. Hence, their cases are similar to our "separate troughs" cases, except that their upper feature is centered at a lower elevation. As do we, they report that westward phase tilt develops. While they don't show growth rates, it seems clear from their Fig. 7a that they also find little growth initially, followed by rapid growth later. They also report that the net growth over time is greatest for an upstream phase tilt of 73° between the surface and 400 hpa. Given the differences in models and initial conditions, their result seems consistent with our Table 1. Our $m = 0.5$ solution corresponds to a shift (between the surface and roughly 200 hpa) of 90°. Somewhere near the value of $m = 0.5$, the growing normal mode attains its largest fraction of the total initial streamfunction.

We have also calculated these quantities for waves which are longer and shorter than the wavelength used in Fig. 2. (The wavelength used in Fig. 2 is close to the most unstable normal mode scale.) We have also examined an isolated wave packet initial condition (the carrier wave being the same as in Fig. 2, but the field is only nonzero over one wavelength). In these cases our basic results are reproduced. NG is greatly weakened by having separate vertical troughs, rather than one sharply tilted trough.

3. Observational evidence

Are observed troughs separate at the start, and if so, what sort of along-flow tilts to they have? Is there evidence of a fixed structure (indicative of NMBI) during some part of the evolution of real storms?

3.1. Caveats

Working with observations presents problems that are not issues in linear dynamics. Two problems are noteworthy to this report. First, the 12 h interval in observations is too long to properly resolve the time evolution of the trough to the extent needed. Whitaker et al. (1988) and Reed et al. (1992) both note this problem. This problem led both groups to use a model simulation in order to obtain sufficient time resolution. We do the same.

A second problem concerns how to identify the location of the trough axis. One might use vorticity (Sanders, 1986). Vorticity fields are quite noisy and it is questionable whether one can implicitly assume that the background vorticity is negligible. Another approach may be to define a perturbation from a time mean. The time mean might be a seasonal one (many winter months), a particular month, or even a period as short as a week (Davis and Emanuel, 1991). We adopted a somewhat different strategy. We chose our cyclogenesis case based upon it's (*in*)sensitivity to the time mean used. That is, we chose our case because (a) a perturbation was clearly identifiable at all levels and (b) the perturbation center was not sensitive to our use of an averaging period between 1 month and 5 days.

Our case study focuses on a storm that forms in the southeastern US on 2 January 1987 and moves up the east coast of the US. Prior to the development, the surface feature was located over the Gulf of Mexico, while the upper level trough was centered over the state of Colorado. Our model is the NCAR CCM2 (Hack et al., 1993) using: T42 horizontal resolution, 18 levels (output interpolated to 10), and all physical parameterizations.

3.2. Separate troughs prior to development?

Most published studies have not been concerned with the vertical tilt of the trough axis in the *along* flow direction. It is more common to find cross sections perpendicular to the trough motion. Whitaker et al. (1988), Davis and Emanuel (1991), and Mass and Schultz (1993) describe upper and lower features that are separate prior to development. Bleck (1990) displays "wire diagram" depictions of three dimensional contours of vorticity in potential temperature coordinates. He does not comment about the tilts, and because the data are presented at 12-h intervals, one cannot deduce phase locking from his charts. In one of Bleck's cases one sees separate upper and lower features each having little tilt; a similar situation is not excluded, but is less clear in his other diagrams.

Fig. 3 shows the trough locations at 3-h time intervals. Two perspectives are used since the trough varies in three dimensions. The upper and lower portions of the trough are approximately vertical at the start. The apparent sharp tilt in the axes between 500–600 and then 600–700 mb levels (during day 1) is an artifact of the plotting scheme used. The scheme connects the centers at successive levels of the largest perturbation at each level. During the first 24 h, at 600 mb there are two distinct centers, one is above the lower trough and one below the upper trough. Over time it is clear that the upper trough is approaching the lower trough and that the upper and lower features move

Tellus A/47/5:1-9

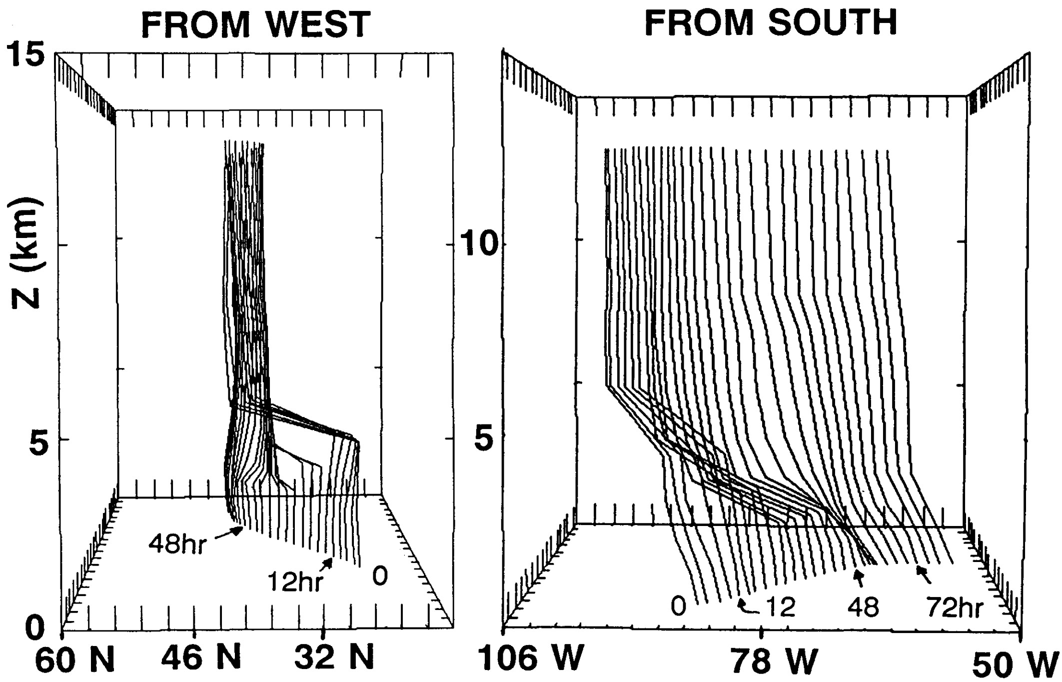

Fig. 3. Trough axis positions at 3-h intervals in CCM2 simulation of observed storm. Period shown: 00 GMT 1 January 1987 (left line) through 12 GMT 4 January 1987 (right line). 9 levels (1000–200 mb) plotted. Plotting scheme connects centers of the deepest trough at each level. An arrow with numeric label at the base of a trough indicates the trough location at the labelled forecast time.

in different directions. Instead of reducing the upstream tilt (as expected for NG), the trough axis is *developing* such a tilt. Most remarkably, for much of the second day in the time simulation, the trough axis structure seems to be *fixed* while propagating. This evolution, including the apparent transient phase locking, is consistent with the theoretical description of a growing normal mode that emerges from a more general initial condition.

Simmons (1994) presents a chart of successive trough axis positions for another frontal cyclone which evolves qualitatively similar to Fig. 3. He remarks that the upper trough that triggers the development has "little phase tilt with height" prior to triggering the development. He also describes the early stage of development as one where "the disturbance moves with a rather uniform phase speed at all heights in a phase-locked manner similar to that of a normal-mode instability."

3.3. Evidence for phase locking?

Before discussing our case study further, some background is useful. Sanders (1986) presents a figure showing the horizontal separation between the vorticity maxima at the surface and 500 mb for 48 instances of explosive cyclogenesis. The data are composited into three categories of storms, and plotted for every 12 h of observations. The distance declines over time in a somewhat regular fashion. Some believe that this figure is strong evidence for the NG mechanism and against the NMBI mechanism. Such conclusions are questionable. First, since only one upper level is used, it is impossible to determine the tilt of the upper trough. As shown above, that tilt is a central issue. Second, since explosive cases are examined the problem with time resolution of the observations is magnified. In other words, the time during which a storm might be approximated by linear dynamics will, by definition, be too short relative to a 12-h time interval. Third, the data are composited. Compositing would make the brief period of NMBI-like behavior (if it exists) even harder to identify, since such behavior would occur at different times relative to the 00 and 12 GMT sampling times. Fourth, if a normal mode is emerging from an upper and a lower feature, tilts must develop in the middle atmosphere. In our theoretical model, the axis at 500 mb approaches the surface axis location for a bit longer after the axis at 200 mb has stopped doing so. (This happens in our observed case, too.) Hence the study by Sanders cannot rule out the NMBI mechanism and does not necessarily contradict what follows.

Some indirect evidence may be found in prior works. Hoskins et al. (1985) present a conceptual model of cyclogenesis whereby an upper level PV anomaly produces a cyclonic circulation at lower levels. If the cyclonic circulation distorts a surface Θ gradient, then an anomaly in surface Θ is also produced. When a surface warm anomaly is produced downstream of the upper level PV anomaly, the two features can reinforce each other. Whitaker et al. (1988) remark that their data are consistent with this conceptual model. They find a lack of development at low levels until the upper level feature arrives at the east coast (just upstream of the surface low), whereupon rapid surface cyclogenesis commences. The upper trough does amplify while approaching the east coast, but one cannot determine the structural changes aloft in the along-flow direction. Davis and Emanuel (1991) examine the relative importance of the three mechanisms described at the start of this

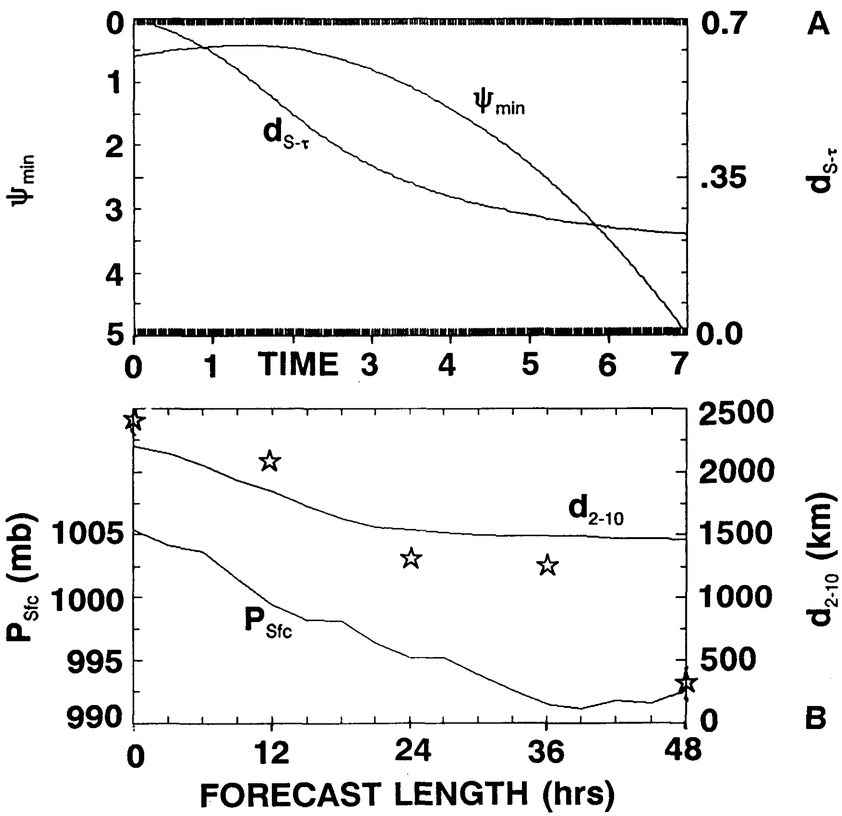

Fig. 4. (a) Linear model time series for the simulation shown in Figs. 2c, d. Distance ($d_{S-\tau}$) between trough positions at surface and tropopause level; minimum surface stream function (ψ_{min}). (b) CCM2 time series. Distance between trough locations at 200 and 1000 mb levels (d_{2-10}). Surface central pressure P_{sfc} in model. Star symbols show observed distances between trough locations at 200 and 1000 mb.

paper by analyzing the development of a frontal cyclone. They find 3 PV anomalies: an upper one (pressure $\leqslant 500$ mb), a lower one (at 850 and 700 mb), and a surface Θ one. By comparing the effects of the anomalies on each other, they find that the upper and surface anomalies reinforce each other and conclude that the mechanism we call NMBI is occurring. They further conclude that the other PV anomaly comes from diabatic processes. The NG mechanism is apparently not strong.

In Fig. 3 we showed trough locations at all levels which provides a general impression of fixed structure for a brief time. To illustrate the structural transition more clearly, one can calculate the separation between the trough location at two levels. In the theoretical model, (Figs. 2c, d) as the growing normal mode emerges, the separation between the upper and lower trough will at first decrease, then asymptote to the phase shift of the normal mode. Fig. 4a shows a time series of the distance between the trough at tropopause and surface levels. This figure also shows the time series of the minimum stream function at the surface; the sequence of little growth or decay followed by exponential growth is evident.

In Fig. 4b, we present the two dimensional distance between the trough center at 200 and at 1000 mb. The behavior is qualitatively similar to the separation change seen in the theoretical model. Surface central pressure is also plotted. Some surface amplification occurs as the separation (d_{2-10}) diminishes (0–21 h). However, amplification continues for the next 18 h even though the separation does not further diminish. In addition, the *observed* separation distance is plotted at the 12-hourly observing times. When compared with the model simulation, it can be argued that the observations also have a brief period of fixed phase. Between 36–48 h, the observed separation again diminishes; the separation (d_{2-10}) in the model simulation also diminishes again after the 48-h period plotted.

4. Conclusions

Our study has focussed on the implications of vertical trough axis tilts to two cyclogenesis mechanisms. Specifically, we emphasize the case where *initially* both a surface trough and an upper level trough upstream have little vertical tilt (i.e., each trough is oriented straight up). Our theoretical results find the NG mechanism to be greatly weakened in this case compared to the situation where the troughs initially are connected (and have larger tilt). As the growing normal mode emerges from the initial condition, the upper and lower troughs become more phase-locked. We examine a particular case of cyclogenesis to show the initial tilts and to see if there is evidence for phase-locking. In our case study we find evidence for both. We examine several published observation-based studies and find evidence which supports what we have shown, especially that presented by Simmons (1994).

5. Acknowledgements

Partial support for this research was provided by UC Davis Hatch funds ID 7601. The authors thank Dr. Y.-H. Lee for calculating the CCM2 forecast output we analyze in Section 3.

REFERENCES

Bishop, C. H. 1993. On the behaviour of baroclinic waves undergoing horizontal deformation. I: The "RT" phase diagram. *Quart. J. Roy. Meteor. Soc.* **119**, 221–240.

Bleck, R. 1990. Depiction of upper/lower vortex interaction associated with extratropical cyclogenesis. *Mon. Wea. Rev.* **118**, 573–585.

Davies, H. C. and Bishop, C. H. 1994. Eady edge waves and rapid development. *J. Atmos. Sci.* **51**, 1930–1946.

Davis, C. A. and Emanuel, K. A. 1991. Potential vorticity diagnostics of cyclogenesis. *Mon. Wea. Rev.* **119**, 1929–1953.

Eady, E. T. 1949. Long waves and cyclone waves. *Tellus* **1**, 33–52.

Farrell, B. 1984. Modal and non-modal baroclinic waves. *J. Atmos. Sci.* **41**, 668–673.

Grotjahn, R. 1980. Linearized tropopause dynamics and cyclone development. *J. Atmos. Sci.* **37**, 2396–2406.

Grotjahn, R., Pedersen, R. and Tribbia, J. 1993. On continuum and normal modes in cyclogenesis. In: *9th Conference on Atmospheric and oceanic waves and stability*. American Meteor. Soc., 31–32.

Grotjahn, R., Pedersen, R. and Tribbia, J. 1994. Linear instability with interior and Ekman friction, Part II: Initial value analysis. *J. Atmos. Sci.* **52**, 764–777.

Hack, J. J., Boville, B. A., Briegleb, B. P., Kiehl, J. T., Rasch, P. J. and Williamson, D. L. 1993. Description of NCAR Community Climate Model (CCM2). NCAR TN-382, 108 pp.

Hoskins, B. J., McIntyre, M. E. and Robertson, A. W. 1985. On the use and significance of isentropic potential vorticity maps. *Quart. J. Roy. Meteor. Soc.* **111**, 877–946.

Mass, C. F. and Schultz, D. M. 1993. The structure and evolution of a simulated midlatitude cyclone over land. *Mon. Wea. Rev.* **121**, 889–917.

Müller, J. C., Davies, H. C. and Schär, C. 1989. An unsung mechanism for frontogenesis and cyclogenesis. *J. Atmos. Sci.* **46**, 3664–3672.

Reed, R. J., Stoelinga, M. T. and Kuo, Y.-H. 1992. A model-aided study of the origin and evolution of the anomalously high potential vorticity in the inner region of a rapidly deepening marine cyclone. *Mon. Wea. Rev.* **120**, 893–913.

Rotunno, R. and Fantini, M. 1989. Petterssen's "type B" cyclogenesis in terms of discrete, neutral Eady modes. *J. Atmos. Sci.* **46**, 3599–3604.

Sanders, F. 1986. Explosive cyclogenesis in the west-central north Atlantic ocean, 1981–84. Part I: Composite structure and mean behavior. *Mon. Wea. Rev.* **114**, 1781–1794.

Simmons, A. 1994. Numerical simulations of cyclone life cycles. In: *The life cycles of extratropical cyclones* **1**, 149–160.

Warrenfeltz, L. L. and Elsberry, R. L. 1989. Superposition effects in rapid cyclogenesis — linear model studies. *J. Atmos. Sci.* **46**, 789–802.

Whitaker, J. S., Uccellini, L. W. and Brill, K. F. 1988. A model-based diagnostic study of the rapid development phase of the president's day cyclone. *Mon. Wea. Rev.* **116**, 2337–2365.